第 48 卷 第 16 期/2021 年 8 月/中国激光 研究论文

中国激光

基于级联拉曼激光倍频的10 W黄光光纤激光器

崔淑珍[1,2]，曾鑫[1,2]，程鑫[1,2]，杨学宗[3]，冯衍[1,3*]

[1]中国科学院上海光学精密机械研究所上海市全固态激光器与应用技术重点实验室，上海 201800；

[2]中国科学院大学，北京 100049；

[3]国科大杭州高等研究院，浙江 杭州 310024

摘要 报道了一种结构紧凑、成本低、稳定性高、操作简单，可应用于皮肤病学及医疗美容领域的黄光激光器。该激光器采用高功率保偏掺镱光纤激光器泵浦级联拉曼嵌套腔的结构，通过使用窄带宽的 1178 nm 光纤布拉格光栅以及优化拉曼增益光纤的长度，获得了高功率窄线宽线偏振 1178 nm 激光。结合基于周期极化钽酸锂晶体的单通倍频方式，实现了 10.19 W 连续波 589 nm 激光的输出，倍频效率为 18.12%。此外，研制的工程样机功率峰峰值浮动小于 2%。

关键词 激光器；光纤激光器；拉曼振荡器；光纤布拉格光栅；非线性光学；二次谐波产生

中图分类号 TN248 **文献标志码** A **doi**：10.3788/CJL202148.1601006

1 引 言

结构紧凑、成本低的高功率 589 nm 激光器在皮肤病学及医疗美容领域具有重要的应用价值，如色素沉着、血管瘤的治疗[1-2]。在皮肤病学中，采用激光治疗血管疾病可追溯到 1960 年，当时使用的是氩离子激光器[3]。1986 年，脉冲染料激光器开始得到了广泛应用[4]。Garden 等[5]通过脉冲染料激光器验证了用 589 nm 激光治疗葡萄酒色斑、血管瘤的有效性。目前，激光手术已成为治疗许多血管病变必不可少的方法。但传统使用的 589 nm 染料激光器具有装置体积大、维护成本高及操作复杂、不便于应用等缺陷，且其本身具有一定的毒性。因此，固态或光纤激光器被广泛应用于医学领域中。

由于缺乏可直接输出 589 nm 激光的高效固体增益介质，目前主要通过对近红外激光进行非线性频率转换实现该波段激光的输出。Jeys[6]提出了一种和频方案，用 1064 nm 和 1319 nm 激光和频产生 589 nm 激光，但该系统的结构复杂，常用于获得大能量黄光激光。Mildren 等[7]采用钨酸钾钆($KGd(WO_4)_2$)晶体将 532 nm 激光拉曼频移获得 589 nm 激光。Yu 等[8]将 1063 nm 激光拉曼频移获得 1173.5 nm 激光，然后倍频输出 586.8 nm 激光。Berger 等[9]用腔内倍频光泵浦半导体获得黄光激光。Yang 等[10]采用 1018 nm 激光泵浦金刚石晶体产生 1178 nm 激光后倍频获得 589 nm 激光。掺镱光纤激光器具有高量子效率、近衍射极限光束质量、热管理方便等优势，近年来得到了飞速发展，可为拉曼激光器提供高功率泵浦源，且在石英光纤透明窗口内的任意波长均可获得拉曼增益。常见的倍频方法有采用外部谐振腔实现高功率、高效率转化[11-13]或采用结构简单的单通倍频方式[14]。Zhang 等[14]将单频拉曼光纤放大器经周期极化钽酸锂(PPSLT)晶体单通倍频后实现了 7 W 的 589 nm 激光输出。Zhang 等[11]采用外腔谐振倍频方式，获得了功率为 50 W 的连续 589 nm 激光，谐振腔腔长采用 Pound-Drever-Hall(PDH)方法进行锁定。但该链路中的反馈控制模块需要精细设计和优化，增加了整个系统的复杂性[15-19]。上述两种方案的基频光均是对单频二极管激光进行两级拉曼放大，且放大

收稿日期：2021-05-27；**修回日期**：2021-06-26；**录用日期**：2021-06-30

基金项目：国家重点研发计划(2020YFB1805900，2018YFB0504600)、上海市科学技术委员会项目(19441909800)

通信作者：*feng@siom.ac.cn

过程中功率受限于受激布里渊散射，无形中增加了系统的成本和复杂性。在医疗领域中应用时，黄光不需要单频，因此，将结构简单的级联拉曼光纤激光器(RFL)和单通二次谐波(SH)产生相结合，可获得高功率连续的黄光激光输出，同时具有实用紧凑的结构和高光束质量等特性。

本文报道了一种结构紧凑、成本低、功率高、线宽窄的黄光激光器，搭建了包层泵浦的高功率线偏振掺镱 1070 nm 光纤激光器泵浦 1120 nm 和 1178 nm 激光的级联振荡腔。将级联拉曼光纤激光器与基于周期极化晶体的单通倍频方式结合，实现了 10.19 W 窄线宽连续黄光激光的输出，其倍频效率为 18.12%。

2 实验装置

激光器的结构如图 1 所示，包括高功率保偏掺镱 1070 nm 光纤激光器，嵌套式级联拉曼光纤振荡腔及单通倍频装置。1070 nm 光纤激光器采用正向泵浦的振荡器结构，泵浦光源为 4 个 60 W 半导体二极管(LD)，中心波长为 976 nm；用合束器将泵浦光耦合进增益光纤。光纤布拉格光栅(FBG)的中心波长为 1070 nm，高反光栅的反射率为 99%，3 dB 反射带宽为 2 nm；低反光栅的反射率为 8%，3 dB 反射带宽为 0.24 nm。增益光纤使用商用 10/125 μm 保偏掺镱光纤(PLMA-YDF-10/125-M)，纤芯直径为 10 μm，在 976 nm 处的包层吸收系数为 4.95 dB/m(4.95 dB/m@976 nm)，数值孔径为 0.075，长度为 6 m。在腔内插入长为 2 m 的单偏振(SP)光纤，通过改变光纤的弯曲半径使快轴光被损耗，腔内只存在慢轴偏振起振，从而实现单偏振激光输出。产生的 1070 nm 激光通过一个 1070/1120 nm 的波分复用器(WDM)耦合进级联拉曼振荡腔，该振荡腔由 1 对波长为 1120 nm 的 FBG、1 对波长为 1178 nm 的 FBG 和 1 段拉曼增益光纤(PM980)组成。为了提高 1120 nm 光到 1178 nm 光的转换效率，1120 nm 的 FBG 反射率均为 99%，1178 nm 高反光栅的反射率为 99%，用于输出耦合的低反光栅反射率为 18%，该嵌套结构可减少拉曼增益光纤的长度，同时提高转换效率。

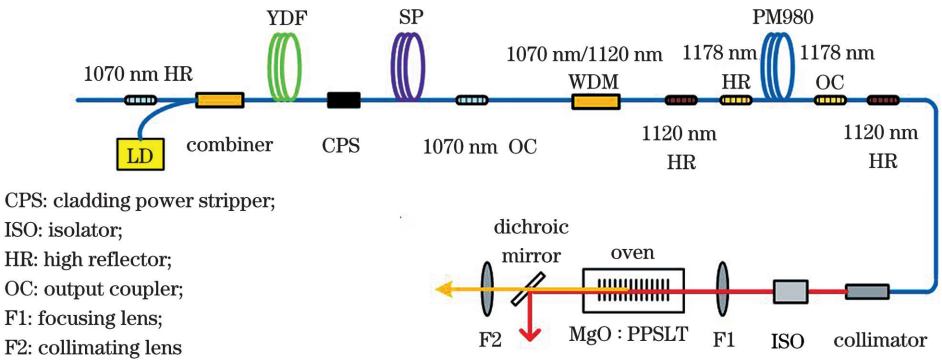

图 1 黄光光纤激光器的结构

Fig. 1 Structure of the yellow fiber laser

输出的拉曼光纤激光经准直后的光斑直径约为 1.3 mm，经光学隔离器后，用焦距为 60 mm 的透镜将光耦合进 PPSLT 晶体。为了减少使用的光学元件，通过旋转准直头匹配隔离器输入偏振的要求，隔离器的输出偏振为垂直偏振，与晶体极化方向平行；隔离器的透过率为 95%。PPSLT 晶体的长为 20 mm，两端均镀有双增透膜(反射率 $R<0.2\%$@1178 nm&589 nm)。将晶体放置在一个自制的晶体炉中，工作温度为 51 ℃，控制精度为 ±0.01 ℃，有利于实现稳定的二次谐波输出。剩余的基频光和产生的倍频光由 45°分光镜分开(透射率 $T>95\%$@589 nm & $R>99.5\%$@1178 nm)。

为了实现高效的二次谐波产生，基频光线宽需尽可能控制在晶体的可接收带宽内，同时需要精确控制倍频晶体的工作温度以及晶体中的光斑大小。计算得到，长度为 20 mm 的 PPSLT 晶体对 1178 nm 基频光的可接收带宽约为 0.2 nm，实验中选用的 1178 nm 输出耦合光栅的带宽为 45 pm，以此获得窄线宽的基频光。计算得到，晶体中的最佳束腰半径为 35 μm，为了避免损坏晶体，实际使用值会略大于最优值。

3 实验结果及分析

1070 nm 激光器输出功率随泵浦光的变化曲线如图 2(a)所示，可以发现，1070 nm 激光的功率随泵浦功率的增加而增加。在最大泵浦功率为 209 W

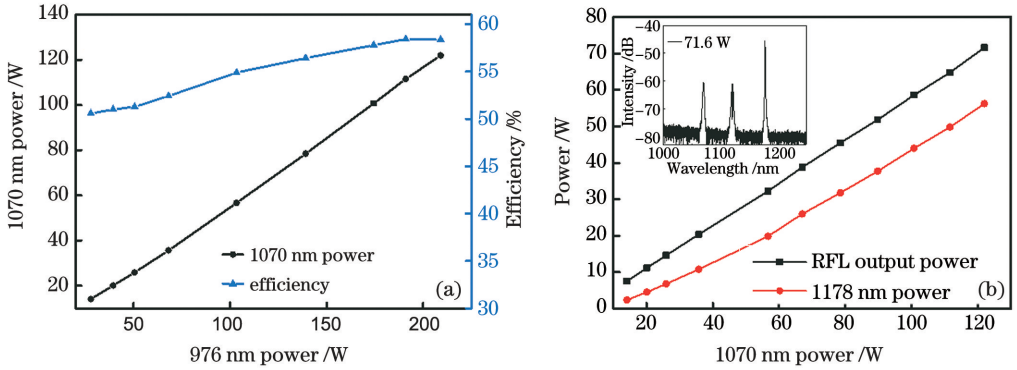

图 2　激光器的输出性能。(a) 1070 nm 激光的功率和转换效率;(b)拉曼激光的总功率及 1178 nm 激光的功率

Fig. 2　Output performance the laser. (a) Power and conversion efficiency of 1070 nm laser; (b) total power of Raman laser and power of 1178 nm laser

时,1070 nm 激光的功率为 122 W,对应的光光转化效率为 58%。在泵浦功率从 191 W 增加到 209 W 的过程中,光光转换效率没有增长。实验过程中,通过优化单偏振光纤的弯曲半径(约为 10 cm),实现了高消光比的线偏振 1070 nm 激光输出,在最高输出功率时,消光比为 20 dB。1070 nm 激光经 WDM 后注入 1120 nm、1178 nm 级联拉曼谐振腔。为提高二阶 1178 nm 拉曼转化的效率,将一阶 1120 nm 拉曼谐振腔设计为高 Q 腔,1120 nm 光栅均为高反光栅。1120 nm 拉曼激光被限制在谐振腔内,通过增强腔内的功率密度将 1120 nm 激光有效转化为 1178 nm 激光。此外,1178 nm 激光的转化效率与激光线宽和拉曼增益光纤的长度有关[20]。实验中测试了长度为 30,40,60 m 光纤的输出特性,虽然增大光纤的长度可提高 1178 nm 激光的转换效率,但光谱展宽更严重,使 589 nm 的倍频输出较小。因此,采用长度为 30 m 的 PM980 光纤作为拉曼增益光纤,并进行了详细的测试与样机研制。由于 1120 nm 和 1178 nm 级联进行拉曼转化,准直头处的输出激光中包含了 1070 nm 残余的泵浦光、1120 nm 一阶拉曼光和 1178 nm 二阶拉曼光。在不同泵浦功率下,各成分激光功率占总输出功率的比例也随之改变,如图 2(b)所示,最高泵浦功率下输出的光谱如图 2(b)中的插图所示。在最大泵浦功率下,总输出功率为 71.6 W,其中,1178 nm 激光的功率为 56.23 W,占比为 78.5%。

随着激光功率的提升,光纤中的热致光栅周期也会发生变化,导致高功率时输出激光的中心波长发生偏移。而倍频过程中基频光的中心波长与倍频晶体的最佳匹配温度有关,进而影响倍频光的转化效率和功率稳定性。实验中,1178 nm 光栅对采用独立的主动温度控制,其中心波长在不同功率下的偏差较小,如图 3(a)所示。可以发现,随着功率的增加,输出光谱逐渐展宽,原因是在高功率拉曼光纤激光器中,光纤中纵模间的四波混频效应会导致输出激光的线宽展宽[21-22],且两翼比中间部分的展宽更明显[23]。为了保证倍频转化效率,基频光的光谱宽度应尽可能地小于倍频晶体的可接收带宽。图 3(b)为 1178 nm 激光在不同功率下的 3 dB 线宽,可以发现,当激光功率为 2.4 W时,线宽约为

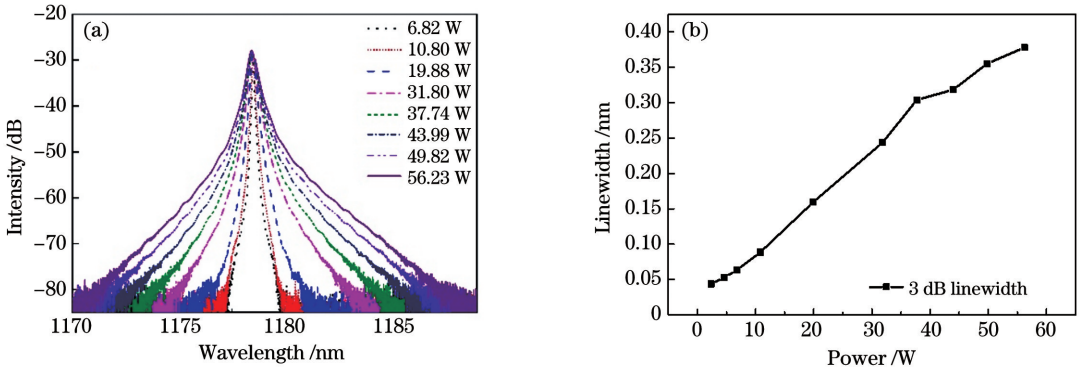

图 3　不同功率下 1178 nm 激光的输出特性。(a)精细谱;(b)3 dB 线宽

Fig. 3　Output characteristics of 1178 nm laser at different powers. (a) Fine spectra; (b) 3 dB linewidth

0.04 nm;在最高输出功率 56 W 时,光谱展宽至 0.38 nm。

准直的 1178 nm 激光经透镜聚焦后单次穿过倍频晶体,采用主动温度控制使倍频晶体稳定在最佳匹配温度(51 ℃),倍频产生的 589 nm 激光功率和二次谐波转换效率随基频光功率的变化如图 4 所示。可以发现,当基频光功率为 56.23 W 时,输出 589 nm 激光的功率为 10.19 W,对应的倍频转换效率为 18.12%。相比文献[24]中单通倍频产生的 509 nm 激光(倍频效率为 20.2%)[24],实验中的基频光光谱展宽导致倍频效率偏低。基频光光谱随激光功率的增加而展宽,在晶体可接收带宽内的光功率占比减少。当基频光功率大于 31.8 W时,其 3 dB 线宽大于 0.24 nm,超过晶体的可接收带宽(0.2 nm),即基频光中可用于有效频率转换的部分减少。但在医疗应用中,10 W 的黄光已基本满足应用需求,且不需要极窄线宽的激光。

将该激光系统进行集成,实现整机输出。在输出功率为 9.5 W 时,进行了 1 h 的功率稳定性测试,结果如图 5 所示,可以发现,功率峰峰值的浮动小于 2%,可采用反馈控制方式进一步提高输出功率的稳定性。由于整个系统中产生和传输基频光的光纤均为单模光纤,因此,经 PPSLT 晶体倍频后获得了近衍射极限光束质量的黄光输出。图 6 为采用光束质量分析仪(M2-200s)测得的 589 nm 激光光束质量,其光束质量因子 M^2 约为 1.05。

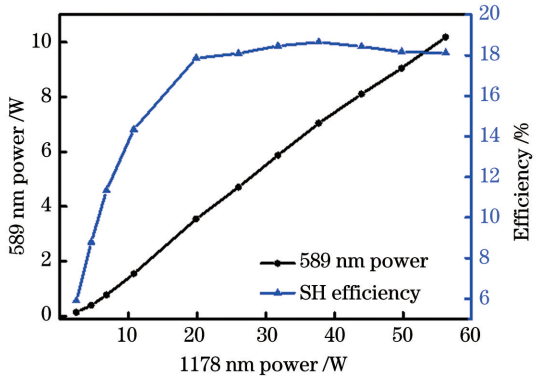

图 4　589 nm 激光的输出功率及倍频效率

Fig. 4　Output power and frequency doubling efficiency of 589 nm laser

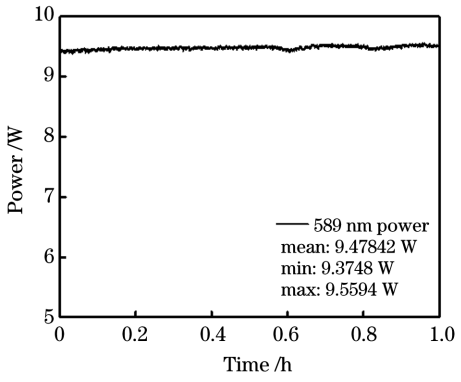

图 5　589 nm 激光功率稳定性

Fig. 5　Power stability of 589 nm laser

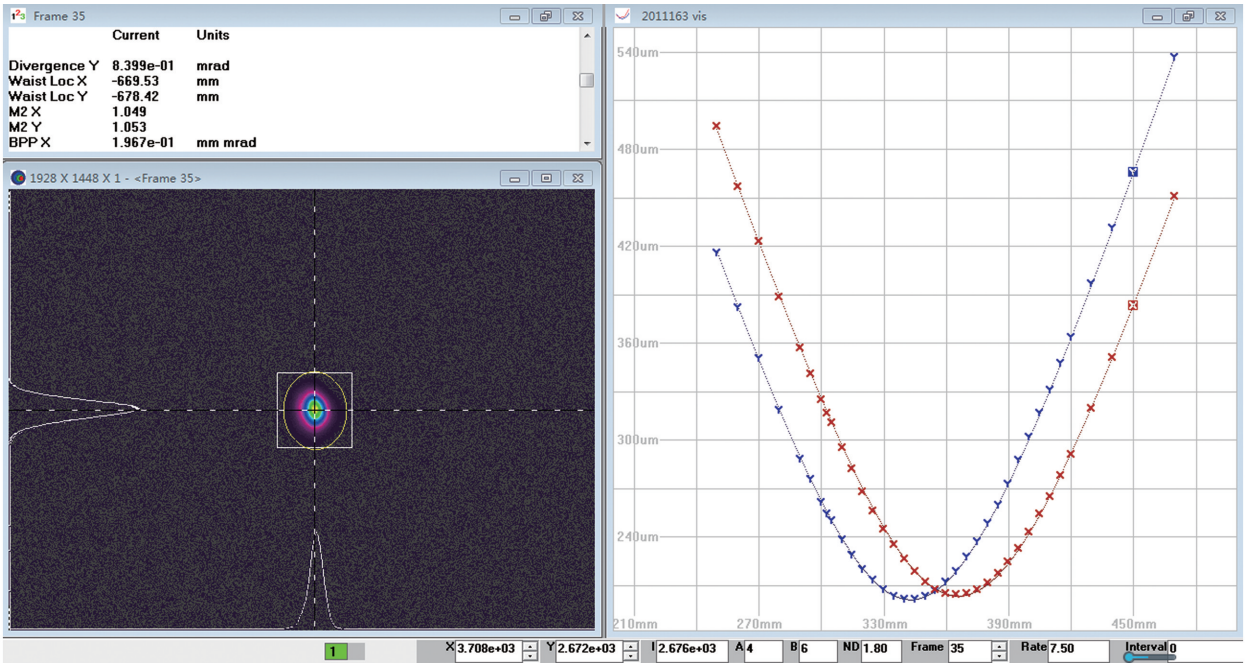

图 6　589 nm 激光的光束质量

Fig. 6　Beam quality of 589 nm laser

4 结 论

针对医疗领域对黄光激光的应用需求，搭建了1070 nm 高功率保偏掺镱光纤激光器，泵浦由1120 nm 和 1178 nm 光栅对组成的级联拉曼振荡腔，以产生 1178 nm 的激光，并分析了高功率窄线宽拉曼光纤激光器的光谱展宽特性及影响线宽的因素。通过优化 1178 nm 光纤光栅的带宽和拉曼增益光纤长度，获得了高功率窄线宽 1178 nm 激光。采用基于 PPSLT 晶体的单通倍频方式，实现了 10.19 W 窄线宽黄光激光输出，并将其集成为工程样机。该激光器具有结构紧凑、成本低、鲁棒性好、操作简单等优点，非常适合应用于皮肤病等医学领域。

参 考 文 献

[1] Carney J A, Gordon H, Carpenter P C, et al. The complex of myxomas, spotty pigmentation, and endocrine overactivity[J]. Medicine, 1985, 64(4): 270-283.

[2] Cheung D S, Warman M L, Mulliken J B. Hemangioma in twins[J]. Annals of Plastic Surgery, 1997, 38(3): 269-274.

[3] Alper T. Cellular radiobiology[J]. Annual Review of Nuclear Science, 1960, 10(1): 489-530.

[4] Lask G, Abergel R P, Dwyer R M, et al. Applications of lasers in dermatology[J]. Proceedings of SPIE, 1986, 0605: 1-4.

[5] Garden J M, Tan O T, Parrish J A. The pulsed dye laser: its use at 577 nm wavelength[J]. The Journal of Dermatologic Surgery and Oncology, 1987, 13(2): 134-138.

[6] Jeys T H. Development of mesospheric sodium laser beacon for atmospheric adaptive optics[C]//LEOS'90. Conference Proceedings IEEE Lasers and Electro-Optics Society 1990 Annual Meeting, November 4-9, 1990, Boston, MA, USA. New York: IEEE Press, 1990: 38.

[7] Mildren R P, Convery M, Pask H M, et al. Efficient, all-solid-state, Raman laser in the yellow, orange and red[J]. Optics Express, 2004, 12(5): 785-790.

[8] Yu H H, Li Z, Lee A J, et al. A continuous wave $SrMoO_4$ Raman laser[J]. Optics Letters, 2011, 36(4): 579-581.

[9] Berger J D, Chilla J L A, Govorkov S, et al. Towards a practical sodium guide star laser source: design for >50 watt LGS based on OPSL[J]. Proceedings of SPIE, 2012, 8447: 84470G.

[10] Yang X Z, Kitzler O, Spence D J, et al. Diamond sodium guide star laser[J]. Optics Letters, 2020, 45(7): 1898-1901.

[11] Zhang L, Jiang H W, Cui S Z, et al. Versatile Raman fiber laser for sodium laser guide star[J]. Laser & Photonics Reviews, 2014, 8(6): 889-895.

[12] Kim J W, Jeong J, Lee K, et al. Efficient second-harmonic generation of continuous-wave Yb fiber lasers coupled with an external resonant cavity[J]. Applied Physics B, 2012, 108(3): 539-543.

[13] Stappel M, Steinborn R, Kolbe D, et al. A high power, continuous-wave, single-frequency fiber amplifier at 1091 nm and frequency doubling to 545.5 nm[J]. Laser Physics, 2013, 23(7): 075103.

[14] Zhang L, Yuan Y, Liu Y H, et al. 589 nm laser generation by frequency doubling of a single-frequency Raman fiber amplifier in PPSLT[J]. Applied Optics, 2013, 52(8): 1636-1640.

[15] Hansch T W, Couillaud B. Laser frequency stabilization by polarization spectroscopy of a reflecting reference cavity[J]. Optics Communications, 1980, 35(3): 441-444.

[16] Drever R W P, Hall J L, Kowalski F V, et al. Laser phase and frequency stabilization using an optical resonator[J]. Applied Physics B, 1983, 31(2): 97-105.

[17] Cui S Z, Zhang L, Jiang H W, et al. 33 W continuous-wave single-frequency green laser by frequency doubling of a single-mode YDFA[J]. Chinese Optics Letters, 2017, 15(4): 041402.

[18] Meier T, Willke B, Danzmann K. Continuous-wave single-frequency 532 nm laser source emitting 130 W into the fundamental transversal mode[J]. Optics Letters, 2010, 35(22): 3742-3744.

[19] Yang X Z, Zhang L, Cui S Z, et al. Sodium guide star laser pulsed at Larmor frequency[J]. Optics Letters, 2017, 42(21): 4351-4354.

[20] Agrawal G. Nonlinear fiber optics [M]. 5th ed. Boston: Academic Press, 2013: 296-298.

[21] Miao Y, Ma P F, Liu W, et al. First demonstration of Co-pumped single- frequency Raman fiber amplifier with spectral-broadening-free property enabled by ultra-low noise pumping[J]. IEEE Access, 2018, 6: 71988-71993.

[22] Liu W, Ma P F, Miao Y, et al. Intrinsic mechanism for spectral evolution in single-frequency Raman fiber amplifier[J]. IEEE Journal of Selected Topics in Quantum Electronics, 2018, 24(5): 1-8.

[23] Liu W, Song J X, Ma P F, et al. Effects of background spectral noise in the phase-modulated

single-frequency seed laser on high-power narrow-linewidth fiber amplifiers[J]. Photonics Research, 2021, 9(4): 424-431.

[24] Qian J P, Zhang L, Jiang H W, et al. 2 W single-frequency, low-noise 509 nm laser via single-pass frequency doubling of an ECDL-seeded Yb fiber amplifier[J]. Applied Optics, 2018, 57(29): 8733-8737.

Generation of 10 W Yellow Fiber Laser by Frequency Doubling of Cascaded Raman Laser

Cui Shuzhen[1,2], Zeng Xin[1,2], Cheng Xin[1,2], Yang Xuezong[3], Feng Yan[1,3*]

[1] *Shanghai Institute of Optics and Fine Mechanics, Chinese Academy of Sciences, Shanghai Key Laboratory of Solid State Laser and Application, Shanghai* 201800, *China*;

[2] *University of the Chinese Academy of Sciences, Beijing* 100049, *China*;

[3] *Hangzhou Institute for Advanced Study, University of Chinese Academy of Sciences, Hangzhou, Zhejiang* 310024, *China*

Abstract

Objective Compact, high-power, low-cost yellow lasers at ~589 nm have potential in dermatological applications. There is no solid-state gain medium that can directly lase at 589 nm, so nonlinear frequency conversion of near-infrared laser is an indispensable technology. The yellow solid laser is usually generated by sum mixing from two Nd∶YAG lasers at 1064 nm and 1319 nm, which the multiple-cavity systems are too complex to use. Yb-doped silica fiber has gain at 1178 nm, but lasing at this wavelength is difficult. So, the Raman fiber laser and amplifier are known for their unique advantage of flexibility in wavelength. The common frequency doubling method employs an external enhancement cavity to achieve high-efficiency and high-power frequency doubling. Nevertheless, it adds complexity to the laser system. In this article, we report a compact, low-cost, high-power, narrow-linewidth yellow laser by single-pass frequency doubling of a cascaded Raman fiber laser in a periodically poled MgO-doped near-stoichiometric $LiTaO_3$ crystal (PPSLT). Up to 10.19-W 589-nm laser is obtained with a conversion efficiency of 18.12%, which is limited by the fundamental laser linewidth. To the best of our knowledge, this laser system has the simplest structure, is the easiest to operate, and is the most suitable for commercial use.

Methods The experimental configuration of the yellow fiber-based laser is shown in Fig. 1, including three functionally different parts—a 1070 nm fiber laser used as a Raman pump source, a cascaded Raman fiber laser, and a single-pass frequency doubling device. The 1070-nm source is a conventional fiber Bragg grating (FBG)-based fiber oscillator. The gain fiber is 10/125-μm polarization-maintaining (PM) Yb-doped fiber (YDF). Using one 1070/1120-nm wavelength division multiplexing (WDM), the generated 1070 nm laser is coupled into the cascaded Raman oscillator, which comprised PM980 gain fiber and two pairs of FBGs with wavelengths of 1120 nm and 1178 nm, respectively. The 1120 nm FBG had a high reflection, which could improve the conversion efficiency from 1120 to 1178 nm. This structure reduced the length of the gain fiber and improved the conversion efficiency. The collimated 1178 nm fiber laser output is optically isolated and focused to incident on a periodically poled MgO-doped near-stoichiometric $LiTaO_3$ crystal (PPSLT). The diameter of the 1178 nm output laser is ~1.3 mm. The length of PPSLT is 20 mm, and the end faces are coated to low reflectivity ($R<0.2\%$) at both 1178 and 589 nm. The PPSLT crystal is installed in a homemade oven operating at 51 ℃ with a control accuracy of ±0.01 ℃. The input polarization of the isolator is matched by rotating the collimator, and the output polarization of the isolator is designed for vertical polarization, which is parallel to the poling direction of the crystal. A dichroic mirror is employed to separate the incident fundamental light and frequency-doubled light, which is highly transmissive at 589 nm ($T>95\%$) and highly reflective at 1178 nm ($R>99.5\%$).

Results and Discussions The CW 1070 nm output power and conversion efficiency are considered as functions of diode pump power. When the diode pump power reaches 209 W, the 1070 nm output power is scaled to 122 W, corresponding to ~58% optical-optical conversion efficiency [Fig. 2 (a)]. The 1070 nm fiber laser is injected into cascaded Raman oscillation cavities. The maximum output power of 1178 nm laser is scaled to 56.23 W

[Fig. 2 (b)]. The central wavelength of the 1178 nm laser is almost the same at different output powers. The 3 dB linewidth of the 1178 nm laser increases with power from 0.04 to 0.38 nm [Fig. 3 (b)], which means the proportion of fundamental light that can be effectively converted is decreasing. The second-harmonic power and second-harmonic generation (SHG) efficiency are considered as functions of the fundamental power at the optimum phase-matching temperature (Fig. 4). When the fundamental power reaches 56.23 W, the maximum SHG output power is 10.19 W, corresponding to a conversion efficiency of 18.12%. The stability of 589 nm laser power measured during 1 h is shown in Fig. 5. Since the fundamental laser is generated with a single-mode fiber and the frequency doubling is achieved with a PPSLT crystal, near-diffraction-limited beam quality is expected (Fig. 6).

Conclusions A 589 nm yellow laser is developed by single-pass frequency doubling of a linearly-polarized narrow-linewidth 1178 nm cascaded Raman fiber laser in a PPSLT. A high-power cladding-pumped Yb-doped 1070 nm fiber laser is built as a Raman pump source. The cascaded Raman process is implemented by 1120- and 1178-nm Raman oscillators. WDM is used in the setup to couple the input pump light and filter the reflected Raman light. Up to 10.19 W continuous-wave 589-nm laser is obtained with a conversion efficiency of 18.12%. The wavelength flexible cascaded Raman fiber laser combined with the single-pass frequency doubling device has advantages of small volume, low cost, good robust performance, and easy operation, which are suitable for use in the medical field.

Key words lasers; fiber lasers; Raman oscillator; fiber Bragg grating; nonlinear optics; second-harmonic generation

OCIS codes 140.3510; 140.3515; 140.3550